High aspect ratio lead zirconate titanate tube structures: II. Directed assembly via dielectrophoresis

Vladimír Kovaľ

Institute of Materials Research SAS, Watsonova 47, 043 53 Košice, Slovak Republic

Received 7 December 2011; received in revised form 9 February 2012; accepted 13 February 2012

Abstract

This paper reports on the controlled manipulation of high aspect ratio ferroelectric microtubes on pre-patterned templates by dielectrophoresis. Microtubes of ferroelectric lead zirconate titanate (PZT, a chemical formula of $Pb(Zr_{0.52}Ti_{0.48})O_3$) with an outer diameter of 2 μm, a length of about 30 μm and a wall thickness of 400 nm were prepared by vacuum infiltration method using macroporous silicon templates. To position and align tubes at designed places, an alternating electric field was applied to a colloidal suspension of PZT tubes through lithographically defined microelectrodes. This would enable creation of a stable electrical connection to individual tubes for making a testing structure for rapid electrical characterization. Electric-field assisted assembly experiments demonstrated that the frequency and magnitude of the applied electric field control dielectrophoretic long-range forces, and hence spatial movement of the tubes in a non-uniform electric field. The most efficient biasing for the assembly of tubes across the electrode gap of 12 μm was a square wave signal of 5 V_{rms} and 10 Hz. By varying the applied frequency in between 1 and 10 Hz, an enhancement in tube alignment was observed due to possible changes in dielectrophoretic torque. The results indicate a great potential for utilizing dielectrophoresis in construction of more complex, hierarchical 3-D device structures using the PZT 1-D like tubes as the building units.

Keywords*: lead zirconate titanate, microtubes, dielectrophoresis, directed assembly*

I. Introduction

Ferroelectric one dimensional (1-D) systems have received considerable attention in the last decade because of their unique properties on the nanoscale and special structure useful in the fabrication of next generations of integrated electronic devices [1–3]. Highly ordered arrays of $Pb(Zr,Ti)O_3$ tube structures with increased electro-active (dielectric and piezoelectric) surface area would enable extreme miniaturization of piezoelectric sensors and actuators, fluidic delivery systems and nonvolatile FeRAM memories [4,5]. These miniaturized devices with size shrinked down to mesoscale dimensions will make it possible to manipulate nano- and microobjects with nano-sized tools, sense force at piconewton scales, induce gigahertz motion and store high densities of information.

High aspect ratio ferroelectric objects of a small size can serve directly as functional elements of miniaturized devices, such as chemical and biological sensors, ink-jet actuators or tunable photonic crystals [1–5]. For the realization of simple planar geometries or more complicated three dimensional (3-D) designs with reliable electrical connections, the development of an appropriate method is required to manipulate and align large quantities of individual 1-D like ferroelectrics. Some useful and efficient approaches have been proposed for insulating and metallic materials, wherein chemical surface treatment, magnetic field, or an electric field is utilized for manipulating micron and sub-micron sized objects [6–8]. However, a selective and controllable assembly of ferroelectric structures with high aspect ratio has not been reported yet. Connecting and interfacing of the small ferroelectrics remotely without direct contact remains a challenge.

One of the most promising candidates for precise positioning and alignment of high aspect ratio nano- and micro-ferroelectrics is dielectrophoresis, which uses an electric field. Dielectrophoresis refers to a translational motion of neutral particles in a suspending me-

* Corresponding author: tel: +421 55 7922464
fax: +421 55 7922408, e-mail: *vkoval@imr.saske.sk*

dium caused by the polarization of the particles in an external non-uniform electric field. The fundamentals of dielectrophoresis and its early applications in biology were introduced by Pohl in 1951 [9]. Since then, the phenomenon has attracted a great interest of nanotechnologists and nanoscientists worldwide and been used for trapping and separation of organic as well as inorganic particles with typical sizes down to the micro- and nanorange. The suitability of the dielectrophoretic technique has been demonstrated for assembling conductive as well as semiconducting carbon nanotubes, CdS and GaN nanowires, ZnO nanostructures, gold nanoparticles and wires [10–14]. The advantages of the electric-field assisted approach in case of ferroelectrics are that a) the electrode array used for directed assembly can serve as a functional electrical connection in electronic devices under operation, b) the position and number density of assembled individuals can be controlled by the adjusting the electric field, and c) the technique is compatible with conventional top-down silicon (Si) micro- and nanomachining techniques, and hence dielectrophoresis offers a powerful tool for batch manufacturing of next generation micro-electro-mechanical system (MEMS) and N(ano)EMS devices.

Usually, dielectrophoresis is performed under an alternating current (AC) sinusoidal field over a wide frequency range. It should, however, be noted that motion of particles has been also observed at very low frequencies [15], indicating that dielectrophoresis occurs in almost direct current (DC) like conditions too. A combination of AC and DC dielectrophoresis was shown very useful in assembling multi-walled carbon nanotubes [16]. It was demonstrated that while DC or low frequency AC electric field can attract the nanotubes to electrodes quickly, a higher frequency electric field provides for an enhancement in tube alignment. Shim *et al.* [17] have recently revealed that AC dielectrophoresis induced by a square wave signal can be very effective in manipulating carbon nanotubes in a low-frequency range (~10 kHz) without the need for a DC signal. Much lower frequencies (~10 Hz) were used by Bowen *et al.* [18,19] for optimum alignment of the PZT fibers and micron sized PZT powders in thermoset polymers.

Besides the frequency of an applied voltage, the dielectrophoretic force depends on a number of other parameters such as the arrangement of the electrodes - electrode shape and gap size; the amplitude of the electric field or the resulting electric field distribution [12,17,20]. Whether the force on the manipulated object is positive (attracting) or negative (repelling) is determined by the polarizability factor, often called as the Clausius-Mossotti factor, whose value mainly depends on the dielectric properties of both the object manipulated and the surrounding medium [21].

In this paper, as an extension of our earlier research on electric-field-assisted manipulation of ferroelectric tube structures with high aspect ratio [22], the ability to assemble as-synthesized PZT microtubes from solution onto pre-patterned electrodes using AC dielectrophoresis is demonstrated. A promising aspect of this research is the possibility to quickly and simply create a stable electrical connection to microtubes at ambient conditions. While the microelectrodes used for tubes alignment can serve directly as bottom electrodes, a deposition of parallel electrodes on top of the assembled tubes would allow for making an electro-active structure for potential applications in high-storage capacitors and high-performance actuators and sensors. The denser upper/bottom electrode structures the larger capacitance or piezoelectricity would be available.

Dielectrophoresis was performed on Ti/Au electrodes with different gap sizes and the influence of the voltage amplitude, waveform and frequency on parallel assembly of PZT tubes was studied and analyzed. It is summarized that careful electrode design and appropriate voltage biasing will allow for arranging ferroelectric microtubes at designed positions with controlled orientation on pre-patterned silicon wafers.

II. Experimental

Highly ordered arrays of polycrystalline PZT microtubes were fabricated by vacuum infiltration method, as described elsewhere [23], using silicon templates with hexagonal two-dimensional pore arrays. Prior to crystallization, an isotropic-pulsed XeF_2 reactive ion etching tool (RIE, Xetch e'series, Xactix Inc., Pittsburgh, PA) was employed to release the tubes from the Si template. This prevents a chemical reaction between silicon and PZT occuring typically at annealing temperatures [23,24], and thereby reduces secondary phase formation in PZT microtubes.

For dielectrophoresis experiments, the 30-μm-long tubes with an outer diameter of 2 μm and a wall thickness of 400 nm were released completely from the template by rinsing in isopropanol (IPA). Then, they were suspended into IPA-filled container by sonification for 5 s. The solution was pipetted onto a pre-patterned silicon wafer. Microelectrodes (Ti/Au = 10/60 nm) were fabricated using electron-beam lithography followed by metal deposition and a standard lift-off procedure. Four different electrode array structures with electrodes gap sizes of 6 μm, 9 μm, 12 μm and 15 μm, respectively, were employed in our experiments. Each electrode array contained a set of 18 alignment sites, each of which has an opposing pair of 240-μm-wide fingers, as shown in Fig. 1.

Figure 2 illustrates schematically an experimental apparatus for manipulation of ferroelectric microtubes through dielectrophoresis. An HP33120A (Hewlett-Packard, Palo Alto, CA) function generator was connected to a voltage amplifier (790 series, AVC Instrumentation) to generate sufficiently large ac elec-

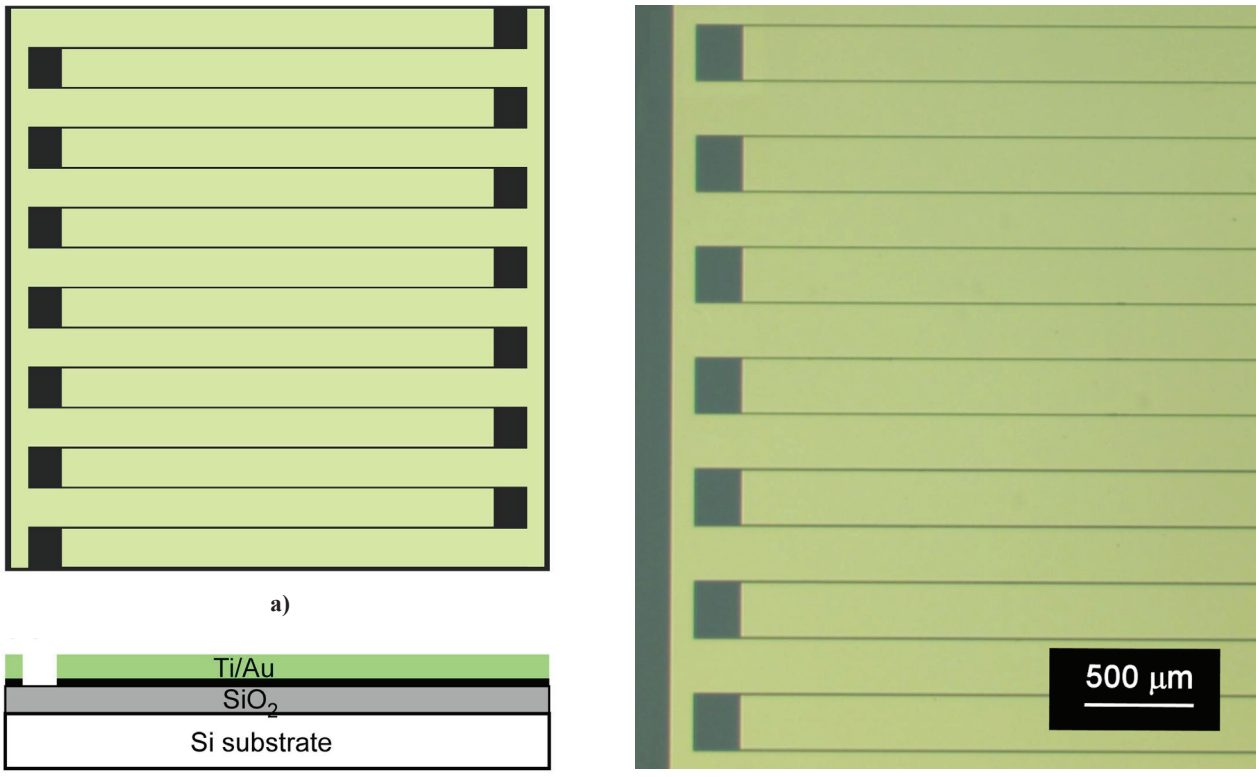

Figure 1. Interdigitated electrode structure used in the dielectrophoretic assembly experiments: (a, b) schematic diagram - top and side view, (c) optical microscope image - top view

tric fields between the electrodes. The sinusoidal and square-wave signals ranging from 1 to 15 V_{rms} were applied at frequencies between 1 Hz and 1 MHz across the microtubes suspension through the two gold microprobes. Each probe can be self-adjusted in the z-axis for a pressure contact setting. The movement of the silicon wafer in the *x-y* direction was carried out with a translation *xy*-stage (Probe Solution Inc., USA). An optical microscope equipped with a CCD camera was used to observe and capture an image of the PZT tubes after electric-field assisted manipulation.

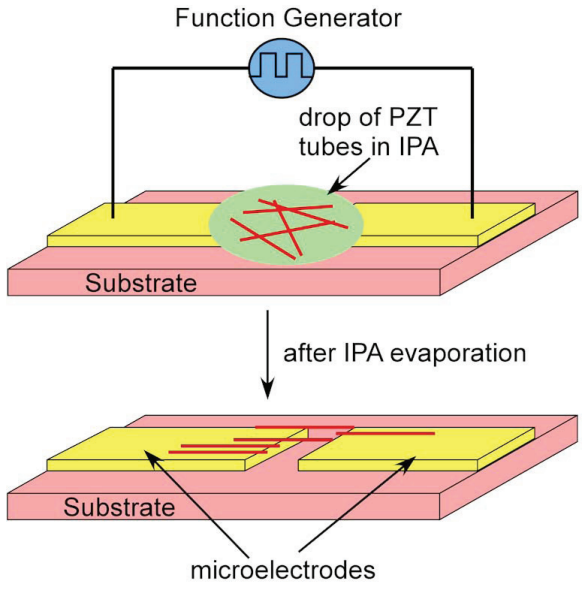

Figure 2. Schematic diagram of the experiment for the electric-field assisted manipulation of microtubes

III. Results and discussion

A representative micrograph of a bunch of the 30 µm long, 2 µm diameter PZT microtubes released from the Si template is shown in Fig. 3. It can be seen from the figure that the tubes are straight, nearly uniform, and completely discrete.

Figures 4a-c show the results from an assembly experiment carried out on with an AC electric field with a RMS (V_{rms}) voltage of 3 V and 5 V (a square wave), respectively, driven at a frequency of 10 Hz. Results are shown for a pair of opposing electrodes, 240 µm wide fingers separated by 12 µm. It can be seen from Fig. 4a that the applied voltage of 3 V_{rms} was not sufficiently large to cause an alignment of tubes. Only a few microtubes near the centre of the electrode gap aligned in the direction of the applied electric field. As the electrode voltage increased to 5 V_{rms}, microtubes, which were deposited and oriented randomly between electrodes at the beginning, aligned in a uniform way and oriented preferentially perpendicular to the direction of the electrodes and parallel to each other. It should also be noted that the tubes appear to be randomly positioned along the electrode length and are mostly touching one of the two adjacent electrodes, as shown in Fig. 4b. The

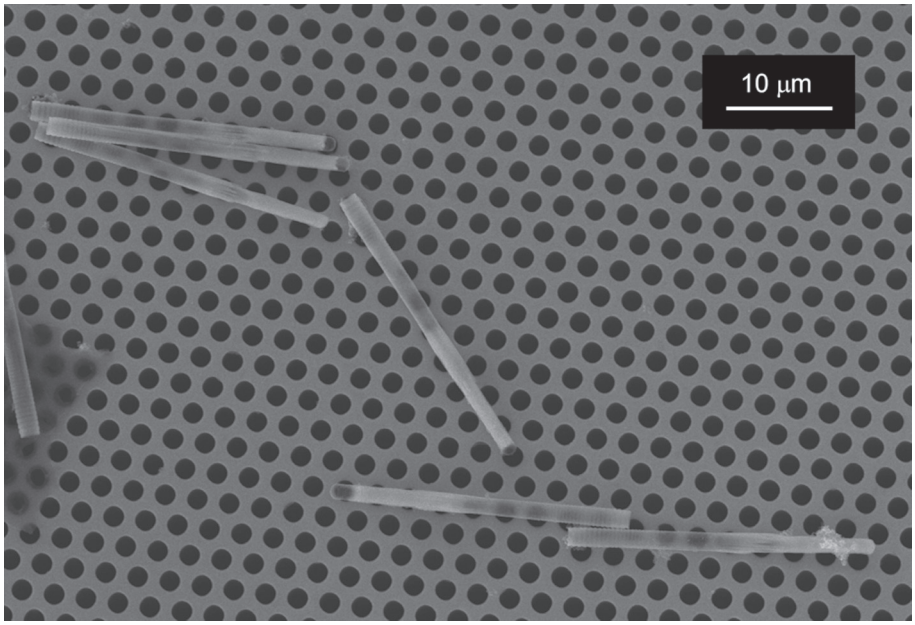

Figure 3. $Pb(Zr_{0.52}Ti_{0.48})O_3$ microtubes released from macroporous silicon template

changes in alignment behaviour caused by a variation in the amplitude of the applied square wave signal are due to forces that induce a translational movement and spatial reorientation of PZT microtubes across the microelectrode array structure and can be rationalized by considering the dielectrophoretic force model [20,21].

When an electric field (E) is applied to a suspension of ferroelectric microtubes, charges accumulate at the interface between the tube and isopropyl alcohol due to Maxwell-Wagner interfacial polarization. As a result, there will be a positive charge induced on one side of the tube and an induced negative charge of the same magnitude on the other side of the tube. The magnitude and direction of the dipole moment (p), induced along the tube, depends on the difference in the polarizability of the tube and the IPA medium. Assuming that the PZT tube is a long prolate spheroid with the longest axis (l) aligned with the electric field, the effective dipole moment can be expressed as [21,25]:

$$\vec{p} = 4\pi r^2 l \varepsilon_m \vec{\alpha} \vec{E} \tag{1}$$

where ε_m is the absolute permittivity of the IPA medium, r is the tube radius, and α is the complex effective polarizability or so called the Clausius-Mossotti factor.

The interaction between the induced dipole moment and a non-uniform electric field produces an unbalanced force (F) on the two poles; the positive charge will experience a pulling force and the negative charge will experience a pushing force, which results in the translational movement of the tube. Generally, the time av-

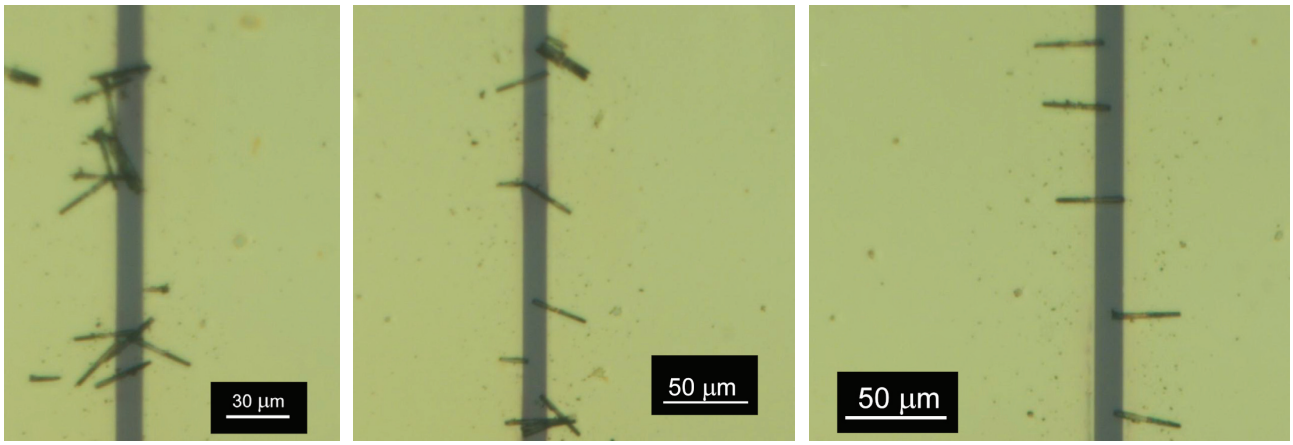

a) **b)** **c)**

Figure 4. Optical microscope images of the selected area of the electrode array with PZT microtubes manipulated within a 12 μm gap by applying a square wave signal of 10 Hz and: a) 3 V_{rms}, b) 5 V_{rms} and c) 5 V_{rms} with rapid frequency variation prior the complete evaporation of isopropanol medium

eraged dielectrophoretic force on an electric dipole in a spatially (and time) dependent electric field is given by [21]:

$$\left\langle \vec{F}_{DEP} \right\rangle = \frac{1}{2} \mathrm{Re}\left[\left(\vec{p}.\vec{\nabla} \right) \vec{E}^{*} \right] \tag{2}$$

where $\vec{E}^{*}$ is the complex conjugate of the electric field.

Combining the above equations, the time averaged dielectrophoretic force experienced by microtubes can be approximated through its first dipole moment contribution (the higher order terms are neglected) as [21,25]:

$$\left\langle \vec{F}_{DEP} \right\rangle = r^2 l \varepsilon_m \, \mathrm{Re}\left[\vec{\alpha} \right] \nabla \left| \vec{E}_{rms} \right|^2 \tag{3}$$

where $\nabla|E_{rms}|^2$ is the gradient of the square of the root-mean-square of the electric field and $\mathrm{Re}[\vec{\alpha}]$ is the real part of the effective polarizability. The gradient is affected by both the geometry of the electrodes and the applied voltage, while as the Clausius-Mossotti factor is a function of the dielectric permittivities and conductivities of microtubes and suspending medium, as well as frequency of the applied AC field [26]:

$$\alpha(\omega) = \frac{\varepsilon_t^{*}(\omega) - \varepsilon_m^{*}(\omega)}{\varepsilon_m^{*}(\omega)} \tag{4}$$

where $\varepsilon^{*} = \varepsilon - j \cdot \sigma/\omega$ is the complex permittivity, ω is the angular frequency of the applied electric field, σ is the conductivity and j is the complex number ($j = \sqrt{-1}$). The subscripts t and m denote tube and medium, respectively.

The accuracy of an Eq. 3 depends on how mirotube size compares to the length of the uniformity of the applied electric field. Liu *et al.* [27] found that when the characteristic length of the electric field is larger than twice the diameter of the spherical particles, the dipole moment approximation estimates the dielectrophoretic force in the direction that is perpendicular to the electrode edges with the relative error within 3 %. As the characteristic length of the electric field increased, the accuracy of the dipole moment approximation improved. When the size of particle is comparable to the characteristic length of the electric field or the spatial field non-uniformity is very large, higher order corrections are needed and multi-pole expansions are necessary. For accurate modelling, Aubry *et al.* [28] used Distributed Lagrangian Method and Maxwell Stress Tensor approach to obtain a solution for the dielectrophoretic force on rigid spherical particles in an electric field cage with spatially disturbed profile.

Following an Eq. 3, the dielectrophoretic force is proportional to the gradient of electric field, $F_{DEP} \propto \nabla E^2$. That means the higher the voltages at a fixed frequency and the same electrode gaps are, the larger the gradients of the electric field intensity and the greater the forces. In this experiment, the force experienced by microtubes at voltages below 5 V_{rms} was not enough to overcome the resistance forces in the solution such as the viscous drag force, gravity or the random thermal force (Brownian motion). A majority of the tubes is loosely pulled and distributed randomly over the entire electrode array. Although, the tubes, which were already close to or in the electrode gaps, were captured between the electrodes by the applied 3-V_{rms}-square-wave signal. This can be explained as a consequence of the nature of the gradient and electric field direction within the electrode structure used [28]. The gradient of the electric field drops off quickly with distance from the electrode. With increasing the electrode voltage up to 5 V_{rms}, the effective force of long-range dielectrophoretic attraction between the tubes and electrodes becomes stronger than the Brownian motion or gravity, resulting in trapping and improved alignment. The force is directed along the gradient of electric field intensity, which is not necessarily aligned with the applied electric field. As a result, PZT tubes may orient and align either along the electric field line or in the direction of the gradient of electric field intensity depending on the applied frequency. Raychaudhuri *et al.* [29] revealed that at low frequencies semiconductor nanowires followed the electric field lines back to one of the two biased electrodes, whereas at higher frequencies the wires were found to move in the direction of the electric field gradient resulting in a greater percentage of nanowires bridging the electrode gap. Our results for ferroelectric microtubes are in agreement with those referred for the low frequency data for InAs nanowires [27,29] and the assembled PZT microtubes are observed only in contact with one of the biased microelectrodes.

Since the field appears as ∇E^2 in Eq. 3, reversing the polarity of the applied voltage does not reverse the force. The numerical sign of F_{DEP} varies with the value of $\alpha(\omega)$ because the complex permittivity spectra of microtubes and isopropyl alcohol are functions of the frequency. In the low and high frequency limits, the real part of the complex polarization factor, Eq. 4, can be simplified as [30]:

$$\mathrm{Re}[\alpha(\omega)] = \begin{cases} \dfrac{\sigma_t - \sigma_m}{\sigma_m}, & \omega \to 0 \\ \dfrac{\varepsilon_t - \varepsilon_m}{\varepsilon_m}, & \omega \to \infty \end{cases} \tag{5}$$

Hence, at very low frequencies ($\omega/2\pi$ < 100 kHz for many practical systems) the dominant electrostatic effect is conduction and the F_{DEP} will depend solely on the conductivity of the PZT tube and suspending IPA medium and is independent of the frequency as well as of the permittivity of the tube and IPA. In the high frequency region, the dielectrophoresis would be dependent on the permittivity of the tube with respect to that of surrounding medium.

For a frequency range, where the real part of the Clausius-Mossotti factor is positive, or where the polarizability of microtubes is higher than that of the surrounding medium, the dielectrophoretic force acting in the direction of the gradient of the electric field is expected to move PZT tubes toward the region of stronger electric field. These areas are, typically, the edges of the planar electrodes [31]. The phenomenon is termed as the positive dielectrophoretic effect. Negative dielectrophoresis with negative values of the effective polarizability factor will take place at frequencies, where the tube is less polarizable than isopropyl alcohol. As a result, the tubes will be pushed to regions corresponding to electric field intensity minima. Since conductivity of the IPA (σ_m = 6 μS/m [13]) at a low frequency is larger than that of a high dielectric PZT, ferroelectric microtubes are expected to experience the negative dielectrophoresis causing their collection at low field points across the electrode array. Figure 4b demonstrates that PZT tubes are pushed towards the regions between two opposing electrodes by the applied 10 Hz electric field.

Some small local perturbations in tube placement and alignment, as observed in Fig. 4b, can be explained by considering (i) an existence of additional surface tension forces associated with an isopropanol evaporation [32], (ii) an unevenness in the distribution of the strength of the dielectrophoretic force caused by the overlapped electric fields from large electrodes [33], and (iii) a variation in dielectrophoretic torque [34].

The dielectrophoretic torque (T_{DEP}) or so called "electrorotation" exerted on a microtube through dielectrophoresis can be expressed in terms of the effective dipole moment approximation as [32]

$$\left\langle T_{DEP} \right\rangle \approx r^2 l \varepsilon_m E_{rms}{}^2 \sin\theta\cos\theta \,\mathrm{Re}\left(\frac{\left(\varepsilon_t^* - \varepsilon_m^*\right)^2}{\varepsilon_m^*\left(\varepsilon_m^* - \varepsilon_t^*\right)} \right) \quad (6)$$

where θ is the angle between the electric field and the longest tube axis.

Liu *et al.* [27] demonstrated using an electrokinetic finite element method that the torque will be always positive and a prolate spheroid will be always driven into alignment with the parallel electrodes terminating in a rectangular shape if the gap size is larger than the length of the spheroid. Wires or tubes longer than the distance between electrodes by two or more times were shown in the analytical model to be misoriented with respect to the microelectrode pair. In addition, Xu *et al.* [33] calculated that the spacing between neighbouring microelectrodes should be larger than twice the width of the electrode to avoid overlapping electric fields and unstable dielectrophoretic forces. These findings coincide with our experimental observation, where several 30-μm-long PZT microtubes are misaligned across the array of 240-μm-wide electrodes with spacing ranging from 2 μm to 15 μm.

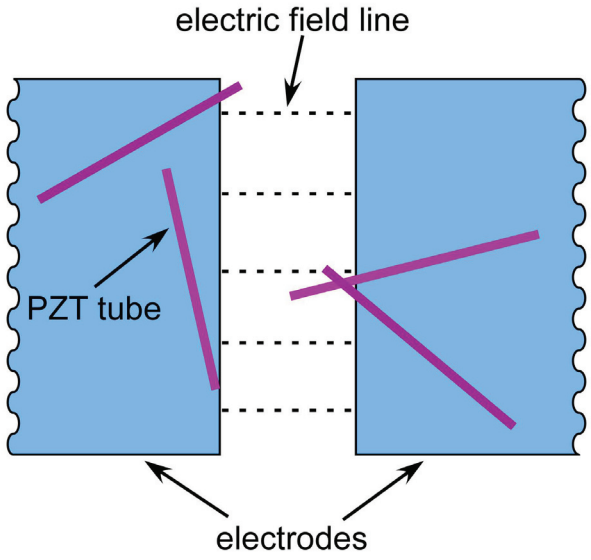

Figure 5a. Conceptual illustration of the frequency variation enhanced alignment (*time: 0–5 s, voltage: 0→5 V_{rms}, freq.: 10 Hz*). At the beginning of the assembly process, the tubes move randomly. They can be trapped with the same probability at any point of the minima of the electric field occurring between two parallel electrodes because the distribution of the electric field is approximately equal along the electrode gaps.

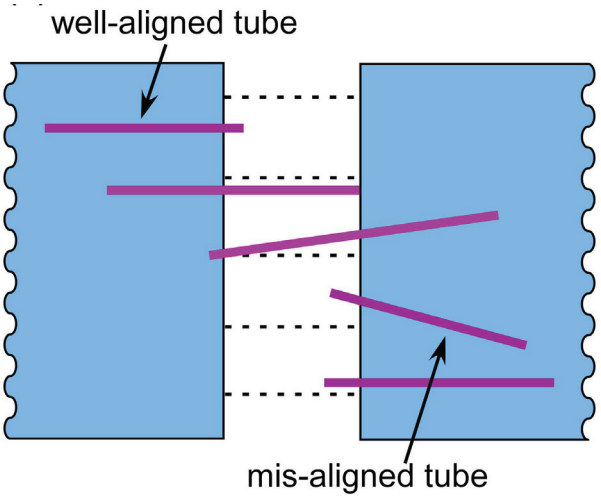

Figure 5b. Conceptual illustration of the frequency variation enhanced alignment (*time: 5–30 s, voltage: 5 V_{rms}, freq.: 10 Hz*). The dielectrophoretic force acting on a microtube is proportional to the gradient of the electric field. Because the gradient of the gradient of the electric field drops off quickly with the distance from the electrode, the dielectrophoretic force acts primarily on microtubes that are close to the electrode gaps. As microtubes approach the electrode gap, large dielectric force induced by dipole-dipole interaction between the electrodes and tube tips leads to trapping of the tubes between the electrodes. A large fraction of the collected tubes are only in contact with one of the electrodes. They are mostly well aligned in the direction of the electric field.

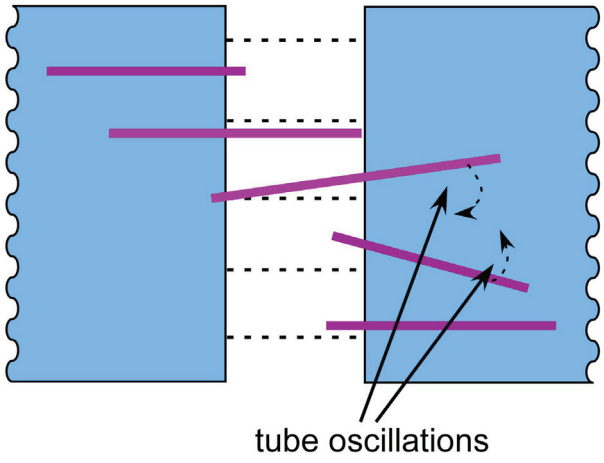

Figure 5c. Conceptual illustration of the frequency variation enhanced alignment (*time: 30-40 s, voltage: 5 V_{rms}, freq.: 1↔10 Hz*). An enhancement in tube alignment was obtained by varying the frequency of the applied rectangular voltage. Upon the frequency variation between 1 and 10 Hz, misaligned tubes were observed to oscillate; while one end of the tube is pivoted, the other end was suddenly freed from its trapped position, rotated and finally re-trapped in a new, energetically more preferable position near the electrode edge with enhanced orientation. By repeating this process several times before the complete evaporation of isopropanol, the overall alignment of the tubes was improved.

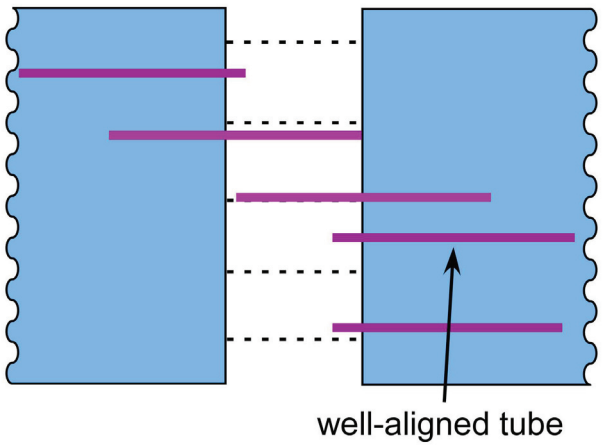

Figure 5c. Conceptual illustration of the frequency variation enhanced alignment (*time: 40 s, voltage: 0, freq.: 0, IPA evaporated*). PZT microtubes assembled between two parallel rectangular shaped electrodes by dielectrophoresis.

The additional degree of tube alignment for the electrode structure used in our dielectrophoresis experiments was achieved at a fixed voltage of 5 V_{rms} by varying the frequency of a square wave between 10 and 1 Hz before the complete evaporation of the IPA. Little field-induced oscillations of a misaligned tube were observed as the frequency was rapidly decreased to 1 Hz. With increasing frequency back to 10 Hz, one end of the tube was suddenly freed, rotated and re-trapped in his new position between the electrodes. We speculate that this effect might be due to the frequency dependant complex polarization factor that causes the changes not only in the dielectrophoretic force but also in the dielectrophoretic torque. Figure 5 shows an illustration of translation and electrorotation of PZT tubes by dielectrophoresis. The result of the repeated re-alignment process is shown in Fig. 5c. It is obvious from the experiment that the overall alignment of the tubes can be improved by a rapid variation of the applied low frequency of a square wave signal.

Increasing the electrode voltage from 5 up to 15 V_{rms} at a fixed frequency of 10 Hz resulted in no tubes trapped in the electrode gaps. The tubes drifted away rather than stayed between the electrodes. This can be explained by increased moving speeds, $v_{DEP} \propto \nabla|E|^2$ [35], at higher electric fields. The effect of a sinusoidal voltage on positioning and aligning of the PZT tubes across the interdigitated electrode structure was found to be ineffective for the investigated amplitudes and frequencies in the range of 1–15 V_{rms} and 10 Hz–1 MHz, respectively. Mechanisms associated with electrohydrodynamic processes generated in suspension of high aspect ratio ferroelectric tube structures by various waveforms need to be further studied. Also, a design of more intricate electrode structures providing spatially confined electric-field profile with greater alignment and capture forces is necessary.

IV. Conclusions

In summary, the results of the electric-field assisted manipulation experiments demonstrate the ability to control the alignment and placement of large numbers of PZT microtubes from solution onto pre-patterned electrodes using dielectrophoresis. Dielectrophoretic behaviour study reveals that most effective electrode biasing for assembling the 30-μm-long microtubes on a 12 μm electrode gap is a rectangular voltage with amplitude of 5 V_{rms} and frequency 10 Hz. A little frequency variation of the applied electric field in the assembled structure with misaligned ferroelectric tubes can improve the overall alignment. It is anticipated that the directed capturing and controlled alignment of high aspect ratio ferroelectric tube structures by an applied electric field would allow for quick and simple creation of stable electrical connections, and hence making a testing structure for rapid electrical characterization. Also, it would facilitate the

fabrication of complicated hierarchical structures for use in miniaturized electronic devices, including piezoelectric MEMS or NEMS, actuators and sensors, and ferroelectric high-density FeRAM memories.

Acknowledgements: This work was partially supported by the Fulbright Commission (Grant No. G-1-00005), the Grant Agency of the Slovak Academy of Sciences (Grant No. 2/0053/11) and COST MP0904 Action. The author would like to thank Professor Susan Trolier-McKinstry and Dr Srowthi Bharadwaja for many stimulating discussions regarding this work and their assistance with material processing, Professor Theresa Mayer and Dr Mingwei Li for electrode design and electrode fabrication.

References

1. J.F. Scott, "Applications of modern ferroelectrics", *Science*, **315** (2007) 954–959.
2. I.I. Naumov, L. Bellaiche, H. Fu, "Unusual phase transitions in ferroelectric nanodisks and nanorods", *Nature*, **432** (2004) 737–740.
3. F.D. Morrison, L. Ramsay, J.F. Scott, "High aspect ratio piezoelectric strontium-bismuth-tantalate nanotubes", *J. Phys.-Condens. Mat.*, **15** (2003) L527–L532.
4. J. Kim, S.A. Yang, Y.Ch. Choi, J.K. Han, K.O. Jeong, Y.J. Yun, D.J. Kim, S.M. Yang, D. Yoon, H. Cheong, K.S. Chang, T.W. Noh, S.D. Bu, "Ferroelectricity in highly ordered array of ultra-thin-walled $Pb(Zr,Ti)O_3$ nanotubes composed of nanometer-sized perovskite crystallites", *Nano Lett.*, **8** (2008) 1813–1818.
5. Y. Luo, I. Szafraniak, N. Zakharov, N. Nagarajan, M. Steinhart, R. Wehrspohn, J.H. Wendorff, R. Ramesh, M. Alexe, "Nanoshell tubes of ferroelectric lead zirconate titanate and barium titanate", *Appl. Phys. Lett.*, **83** (2003) 440–442.
6. D.P. Long, J.L. Lazorcik, R. Shashidhar, "Magnetically directed self-assembly of carbon nanotube devices", *Adv. Mater.*, **16** (2004) 814–819.
7. S.G. Rao, L. Huang, W. Setyawan, S. Hong, "Large-scale assembly of carbon nanotubes", *Nature*, **425** (2003) 36–37.
8. Ch.P. Luo, A. Heeren, W. Henschel, D.P. Kern, "Nanoelectrode arrays for on-chip manipulation of biomolecules in aqueous solutions", *Microelectron. Eng.*, **83** (2006) 1634–1637.
9. H.A. Pohl, "The motion and precipitation of suspensoids in divergent electric fields", *J. Appl. Phys.*, **22** (1951) 869–871.
10. P.A. Smith, Ch.D. Nordquist, T.N. Jackson, T.S. Mayer, B.R. Martin, J. Mbindyo, T.E. Mallouk, "Electric-field assisted assembly and alignment of metallic nanowires", *Appl. Phys. Lett.*, **77** (2000) 1399–1401.
11. R. Krupke, F. Hendrich, H.V. Lohneysen, M.M. Kappes, "Separation of metallic from semiconducting single-walled carbon nanotubes", *Science*, **301** (2003) 344–347.
12. S.Y. Lee, T.H. Kim, D.I. Suh, N.K. Cho, H.K. Seong, S.W. Jung, H.J. Choi, S.K. Lee, "A study of dielectrophoretically aligned gallium nitride nanowires in metal electrodes and their electrical properties", *Chem. Phys. Lett.*, **427** (2006) 107–112.
13. S.Y. Lee, A. Umar, D.I. Suh, J.E. Park, Y.B. Hahn, J.Y. Ahn, S.K. Lee, "The synthesis of ZnO nanowires and their subsequent use in high-current field-effect transistors formed by dielectrophoresis alignment", *Physica E*, **40** (2008) 866–872.
14. S. Kumar, S.H. Yoon, G.H. Kim, "Bridging the nanogap electrodes with gold nanoparticles using dielectrophoresis technique", *Curr. Appl. Phys.*, **9** (2009) 101–103.
15. S. Rajaraman, H.S. Noh, P.J. Hesketh, D.S. Gottfried, "Rapid, low cost microfabrication technologies toward realization of devices for dielectrophoretic manipulation of particles and nanowires", *Sensor Actuat. B-Chem.*, **114** (2006) 392–401.
16. X.Q. Chen, T. Saito, H. Yamada, K. Matsushige, "Aligning single-wall carbon nanotubes with an alternating-current electric field", *Appl. Phys. Lett.*, **78** (2001) 3714–1716.
17. H.Ch. Shim, Y.K. Kwak, Ch.S. Han, S. Kim, "Effect of a square wave on an assembly of multi-walled carbon nanotubes using AC dielectrophoresis", *Physica E*, **41** (2009) 1137–1142.
18. C.P. Bowen, T.R. Shrout, R.E. Newnham, C.A. Randall, "A study of the frequency dependence of the dielectrophoretic effect in thermoset polymers", *J. Mater. Res.*, **12** (1997) 2345–2355.
19. C.P. Bowen, R.E. Newnham, C.A. Randall, "Dielectric properties of dielectrophoretically assembled particulate-polymer composites", *J. Mater. Res.*, **13** (1998) 205–210.
20. H.A. Pohl, *Dielectrophoresis*, Cambridge University Press, Cambridge, 1978.
21. T.B. Jones, *Electromechanics of Particles*, Cambridge University Press, New York, NY, 1995.
22. V. Koval, S.S.N. Bharadwaja, M. Li, T.S. Mayer, S. Trolier-McKinstry, "Dielectrophoretic assembly of lead zirconate titanate microtubes", *Solid State Commun.*, **151** (2011) 1990–1993.
23. V. Koval, "High aspect ratio lead zirconate titanate tube structures: I. Template assisted fabrication - vacuum infiltration method", *Process. Applic. Ceram.*, **6** [1] (2012) 37–42.
24. S.S.N. Bharadwaja, M. Olszta, S. Trolier-McKinstry, X. Li, T. Mayer, F. Roozeboom, "Fabrication of high aspect ratio ferroelectric microtubes by vacuum infiltration using macroporous silicon templates", *J. Am. Ceram. Soc.*, **89** (2006) 2695–2701.
25. R.H.M. Chan, C.K.M. Fung, W.J. Li, "Rapid assembly of carbon nanotubes for nanosensing by dielectrophoretic force", *Nanotechnol.*, **15** (2004) S672–S677.
26. H. Morgan, N.G. Green, "Dielectrophoretic manipulation of rod-shaped viral particles", *J. Electrost.*, **42** (1997) 279–293.

27. Y. Liu, J.H. Chung, W.K. Liu, R.S. Ruoff, "Dielectrophoretic assembly of nanowires", *J. Phys. Chem. B*, **110** (2006) 14098–14106.
28. N. Aubry, P. Singh, "Control of electrostatic particle-particle interactions in dielectrophoresis", *Europhys. Lett.*, **74** (2006) 623–629.
29. S. Raychaudhuri, S.A. Dayeh, D. Wang, E.T. Yu, "Precise semiconductor nanowire placement through dielectrophoresis", *Nano Lett.*, **9** (2009) 2260–2266.
30. M. Dimaki, P. Bøggild, "Dielectrophoresis of carbon nanotubes using microelectrodes: a numerical study", *Nanotechnol.*, **15** (2004) 1–8.
31. N. Crews, J. Darabi, P. Voglewede, F. Guo, A. Bayoumi, "An analysis of interdigitated geometry for dielectrophoretic particle transport in micro-fluidics", *Sensor Actuat. B-Chem.*, **125** (2007) 672–679.
32. W.J. Liu, J. Zhang, L.J. Wan, K.W. Jiang, B.R. Tao, H.L. Li, W.L. Gong, X.D. Tang, "Dielectrophoretic manipulation of nano-materials and its application to micro/nano-sensors", *Sensor Actuat. B-Chem.*, **133** (2008) 664–670.
33. D. Xu, A. Subramanian, L. Dong, B. J. Nelson, "Shaping nanoelectrodes for high-precision dielectrophoretic assembly of carbon nanotubes", *IEEE T. Nanotechnol.*, **8** (2009) 449–456.
34. C.Y. Yang, U. Lei, "Dielectrophoretic force and torque on a sphere in an arbitrary time varying electric field", *Appl. Phys. Lett.*, **89** (2006) 163902.
35. N.G. Green, A. Ramos, H. Morgan, "Ac electrokinetics: a survey of sub-micrometre particle dynamics", *J. Phys. D Appl. Phys.*, **33** (2000) 632–641.